Stereo-Dynamics of Autoionization Reactions Induced by $Ne^*(^3P_{0,2})$ Metastable Atoms with HCl and HBr Molecules: Experimental and Theoretical Study of the Reactivity Through Selective Collisional Angular Cones

Marco Parriani[1], Franco Vecchiocattivi[1], Fernando Pirani[1,2], and Stefano Falcinelli[1(✉)]

[1] Department of Civil and Environmental Engineering, University of Perugia, Via G. Duranti 93, 06125 Perugia, Italy
franco@vecchio.it, {fernando.pirani,stefano.falcinelli}@unipg.it
[2] Department of Chemistry, Biology and Biotechnologies, University of Perugia, Via Elce di Sotto 8, 06100 Perugia, Italy

Abstract. In this paper are presented mass spectrometric determinations as a function of the collision energy in the 0.03–0.50 eV range as recorded in a crossed molecular beam experiments involving autoionization reactions between $Ne^*(^3P_{2,0})$ metastable atoms and HCl and HBr molecules. The total and partial ionization cross sections for both investigated systems are presented and discussed in a comparative way. The comparison of the recorded data allows to point out similarities and differences on the collisional stereodynamics of $Ne^*(^3P_{0,2})$-HCl and $Ne^*(^3P_{0,2})$-HBr systems. In particular, an accurate characterization of the interaction potentials, which is mandatory for a comprehensive description of Ne^*-HX (X = Cl and Br) reactive collisions, has been outlined. Such a theoretical analysis suggests that the formation of the proton transfer, NeH^+, ions as well as of other possible product ions (i.e. HX^+ and $NeHX^+$, parent and associate ions, respectively) comes from reactivity that is selectively open along angular cones showing different orientation and acceptance. In particular, the performed analysis highlights that the proton transfer rearrangement reaction, which is open in both Ne^*-HX autoionizing collision, is much more efficient for Ne^*+HCl respect to Ne^*+HBr autoionization. The present investigation points out that such an efficiency variation is related to the following crucial points: (i) the different charge distribution on HX^+ ionic products, (ii) the balance between two distinct microscopic mechanisms that are operative in such processes (a pure physical-photoionization-indirect mechanism and a chemical-oxidation-direct mechanism), which are reactions of interest in combustion chemistry, plasma physics and chemistry, as well as in astrochemistry and for the chemistry of planetary ionospheres.

Keywords: Autoionization · Stereo-dynamics · Proton transfer · Charge transfer · Transition state · Mass spectrometry · Astrochemistry

© The Author(s), under exclusive license to Springer Nature Switzerland AG 2022
O. Gervasi et al. (Eds.): ICCSA 2022 Workshops, LNCS 13378, pp. 270–280, 2022.
https://doi.org/10.1007/978-3-031-10562-3_20

1 Introduction

In general, autoionization reactions, also named Penning ionization or chemi-ionization processes [1–4], are relevant in different fields of scientific research, as combustion chemistry, plasma physics and chemistry, as well as in astrochemistry and in ionosphere of Planets where they have an effect on the transmission of radio and satellite signals [5, 6]. More recently, from a fundamental point of view these processes have attracted the attention of the scientific community interested in studying the characteristics of quantum resonances present in reactive and non-reactive collisions. Such an important research topic has been addressed and developed using the molecular beams technique performed under ultra-cold conditions through very advanced and frontier experiments able to simulate what happens from a chemical point of view in interstellar environments [7].

Chemi-ionizations are well-known elementary gas-phase reactions which imply neutral reagents able to generate more stable ionic species. They are very common in nature and take place in numerous environments of chemical interest. In particular, these reactions are relevant in combustion chemistry, since are considered as primary steps in flames [8, 9].

When chemi-ionizations involve reagent species in an internally excited metastable state as ionizing agent of atomic or molecular targets, we commonly refer to collisional autoionization or Penning ionization processes. The reader interested in a general overview of these processes can refer to various review articles already published [2, 3].

When we consider autoionization reactions involving electronically excited metastable species (this is the case of noble gas atoms, Ng, excited in their first electronic level), our research group demonstrated that a general semiempirical model can be applied for their description. In fact, very recently, we developed an original and innovative theoretical approach which allow a simple and general rationalization and representation of chemi-ionizations as prototype elementary oxidation processes [10–12]. In our model, we can schematize this kind of processes by the Eq. (1) below:

$$\begin{aligned} Ng^* + X \rightarrow (Ng \cdots X)^* \rightarrow (Ng \overset{e^-}{\leftarrow} X)^* \rightarrow \\ (Ng \cdots X)^+ + e^- \rightarrow \text{ion products} \end{aligned} \tag{1}$$

where, Ng^* is a Noble gas open-shell atom, in an electronically excited metastable state, which collides with the X target being an atomic or molecular species. In this case, the collision leads to the generation of a collision complex $(Ng\cdots X)^*$ in an excited energetic state which relaxes its excess of energy via an electron emission [2, 3], as shown in Eq. (1). $(Ng\cdots X)^*$ is the precursor state of the process with an electron excited in a high energetic Rydberg state. For such barrierless reactions it represents the transition state which, under thermal collisions, gives rise to the formation of ionic products: X^+ (parent ion), NgX^+ (associated ionic aggregates), as well as dissociated or rearranged ions. This occurs by an oxidation process which is schematized in Eq. (1) by the left-going arrow representing an electron exchange between the collisional target X and the core of Ng^*.

The autoionization processes involving Ng^* + HCl and HBr molecules have attracted great interest from various researcher groups during last forty years, since they are important for the development of excimer lasers. In fact, the chemi-ionization reactions generated by collision with $Ne^*(^3P_{0,2})$ metastable atoms are important processes occurring in the formation of the $XeCl^*$ excimer molecule which is produced in Xe + HCl gaseous

mixtures discharge containing an excess of Ne. Due to this considerable scientific interest, a number of valuable articles have been published on this topic since the 1980s, either from a theoretical [13–16] and an experimental point of view [17–24].

This paper reports on mass spectrometric determinations as a function of the collision energy in the range of 0.03–0.50 eV for $Ne^*(^3P_{0,2})$-HCl and $Ne^*(^3P_{0,2})$-HBr autoionization processes. The experimental study was performed using a crossed molecular beams apparatus allowing the measure of the total and partial cross sections for all the open ionization channels in the investigated energy range. In order to highlights similarities and differences in the collisional stereodynamics of the two systems, new data recorded for Ne^*-HBr chemi-ionization are analyzed and discussed in comparison with the previous ones obtained for Ne^*-HCl system [23, 24]. With this procedure, we were able to rationalize the behavior of the two Ne^*-HX (X = Cl, Br) systems in term of the main physical properties of the interaction potentials involved in the reactive collisions. This was possible taking into account of the results recorded in other laboratories and obtained in Penning ionization electron spectroscopy (PIES) studies previously performed either by Hotop and coworkers [25, 26] and by Ohno group [27].

Previous mass determinations on Ne^*- HCl chemi-ionization performed in our laboratory showed the formation of the following ionization channels at an averaged collision energy of 45 meV:

$$Ne^* - HCl \rightarrow Ne + HCl^+ + e^- \qquad (\approx 87\%) \tag{2}$$

$$\rightarrow \; NeH^+ + Cl + e^- \qquad (\approx 10.5\%) \tag{3}$$

$$\rightarrow \; NeHCl^+ + e^- \qquad (\approx 2.5\%) \tag{4}$$

Very interesting was the formation of the protonated neon ion, NeH^+ coming out from a chemical proton transfer reaction between the colliding reagents. Furthermore, experiments aimed to investigate the isotopic effect have been performed studying by mass spectrometry the chemi-ionization of DCl induced by Ne^* atoms. Such an experiment pointed out a statistical character of the proton transfer process that was confirmed by theoretical calculations performed by SCF, CI, and CASSCF methods [23]. In this paper we extend such an analysis to the Ne^*-HBr chemi-ionization in order to achieve a complete understanding of such autoionization reactions. In particular, we are able to emphasize that the reaction channels, leading to the formation of parent HCl^+ or HBr^+ ions in ground and excited electronic states, of associated ($NeHCl^+$ and $NeHBr^+$) ions and of NeH^+ proton transfer species, are opened along most suitable angular cones having specific orientation and acceptance.

2 Theoretical and Computational Approach

The theoretical and computational approach employed for atom-molecules autoionization processes is founded on the so called Optical Potential Model (OPM) introduced first in 1940 by Hans Bethe [28]. In this model is adopted a complex potential W in order to fully describe the intermolecular potential microscopic autoionization dynamics according to the following equation:

$$W = V - \frac{i}{2}\Gamma \tag{5}$$

V is the real part of the complex potential able to simulate the Ng^* - X collisional interaction during the approach of the reacting partners, while Γ is an imaginary function of such a OPM that can be used for a proper quantification of the autoionization probability through which the intermediate collisional complex $(Ng\text{---}X)^*$ (i.e., the transition state of the autoionization reaction) evolves toward the formation of the final ion products [29–32].

In our laboratory we have developed a new semiclassical treatment which was recently applied to various atom-atom autoionization processes [33, 34]. In these studies, for the first time the real and the imaginary part of OPM were treated as two considered interdependent analytical functions, following the general treatment whose details can be found by the reader in refs. [11, 12] where are also highlighted differences and peculiarities respect to previous computational models commonly used to treat from a theoretical point of view autoionization reactions [35, 36]. In this model, we are able to clarify that autoionization reactions are prototype of simple oxidation processes and can involve two different microscopic reaction mechanisms: (i) at low energy collision, high internuclear distances are probed by the reacting partners and a typical photo-ionization (physical) mechanism is the responsible of the production of final ions (*indirect mechanism*); (ii) for collision energy in the thermal or hyper-thermal regime a real oxidation (chemical) mechanism become prominent through an electron transfer between Ng^* and X (*direct mechanism*) as is showed in Eq. (1) [12]. Furthermore, our semiclassical treatment allowed to obtain a clear physical description of the reactive collision highlighting the direct relation between the angular momentum couplings by Hund's cases and the selectivity of the electronic rearrangements which trigger the two *direct* and *indirect* microscopic mechanisms mentioned above [33].

In this paper, we apply our computational treatment in the analysis of the total and partial ionization cross sections obtained in experiments performed using a beam of $Ne^*(^3P_{0,2})$ as an ionizing agent of HCl and HBr molecules. Our theoretical description is useful not only to understand the behavior of either total ionization cross sections and branching ratios of ionic products, but also to evaluate the more probable orientation of the Ng^*-HX (X = Cl and Br) reagents in their preferential reactive angular cones, establishing if and when the involved intermolecular electric field gradients (owing to anisotropic intermolecular forces) are effective. For this latter purpose we used the same theoretical approach successfully applied in the case of autoionization reactions involving other hydrogenated molecules as H_2O, NH_3 and H_2S [37, 38].

3 Cross Section Measurements

The measurements of total and partial ionization cross sections as well as of branching ratios of various accessible ionization channels following the autoionization between $Ne^*(^3P_{0,2})$ metastable atoms and the molecular HX targets have been performed using mass spectrometry technique coupled with a molecular beam apparatus. This prototype high vacuum machine, is composed by three differentially pumped vacuum chambers

able to study the microscopic stereodynamics of autoionization processes in a single collision condition, since operating at about 10^{-7} mbar. Such an apparatus consists of a primary chamber which is the one where the rare gas metastable atoms can be generated using two kinds of sources: (i) an electron bombardment device working at about 150 eV; (ii) a microwave discharge using a brass (water-cooled) resonant cavity working at 2450 MHz and 70–200 kW as typical operating power range.

In the second vacuum chamber, the primary beam of metastable atoms so produced is analyzed in its velocity distribution using the time of flight (TOF) technique by means of a TOF disk: this technique is used to record mass spectra and cross sections as a function of the collision energy that are the physical observables presented in this paper.

The scattering chamber is the third one, hosting the crossed molecular beams volume (which crosses at right angle) and the two diagnostic devices allowing the detection of product ions and the kinetic energy of emitted electrons from the transition state of the studied reactions. For the first measurements, a quadrupole mass filter is used and is located below the scattering volume. For the latter kind of measurements, an electron energy analyzer, placed above the crossed molecular beams allows the so-called Penning Ionization Electron Spectroscopy (PIES) measurements, obtaining a real spectroscopy of the transition state for such processes. The experimental apparatus is schematized in Fig. 1 and is fully described elsewhere [39–41].

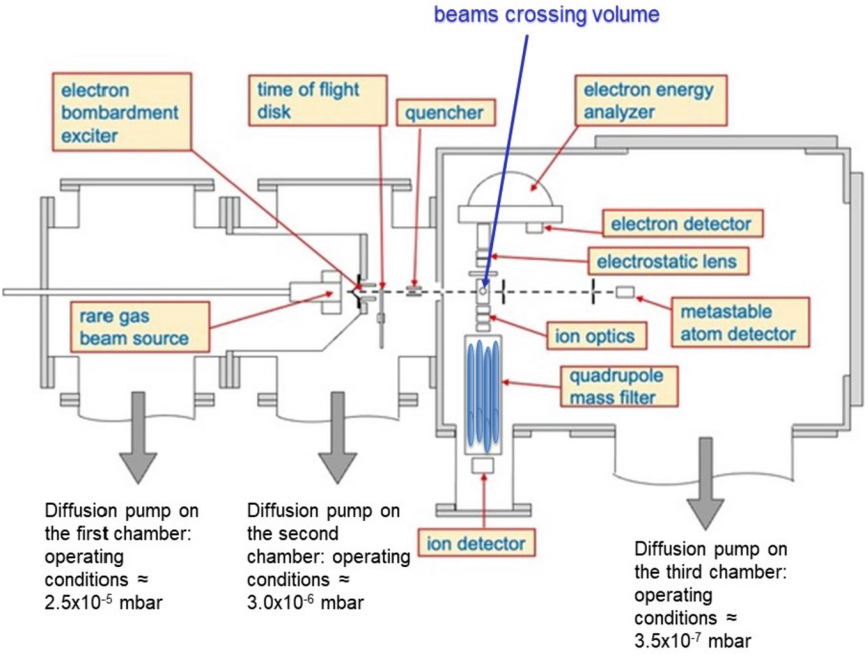

Fig. 1. The scheme of the prototype apparatus operating in the laboratory of Perugia. It consists of two molecular beams crossing at right angle in the third vacuum chamber (see the right side of the figure). Left side: the first vacuum chamber hosting the source of metastable rare gas atoms. The second vacuum chamber is shown in the central part of the diagram: here the velocity selection of the metastable atomic beam is performed by TOF technique. Detectors of the metastable rare gas atom beam and of ion products are channel electron multipliers (CEM) are located in the scattering chamber (on the right) together the quadrupole mass filter and the electron energy analyzed which are the used diagnostic techniques.

4 Results and Analysis

Mass spectrometric determinations on $Ne^*(^3P_{0,2})$-Br autoionizing collisions recorded in the collision energy range of 30–500 meV showed the possible formation of HBr^+ Penning ions, $NeHBr^+$ associative ionization and NeH^+ ions produced by a proton transfer reaction between the collisional partners. The relative abundances for each open ionization channels, as determined at an averaged collision energy of 45 meV, are reported below:

$$Ne^* - HBr \rightarrow Ne + HBr^+ + e^- \qquad (\approx 96.6\%) \tag{6}$$

$$\rightarrow NeH^+ + Cl + e^- \qquad (< 1.0\%) \tag{7}$$

$$\rightarrow NeHBr^+ + e^- \qquad (\approx 2.7\%) \tag{8}$$

From the mass spectra recorded as a function of the collision energy, we have determined the total ionization cross sections and the branching ratios for the possible ionization open channels. Such data are collected for the two Ne^*-HX (X = Cl and Br) systems in the same experimental conditions and are shown in Fig. 2 in a comparative way.

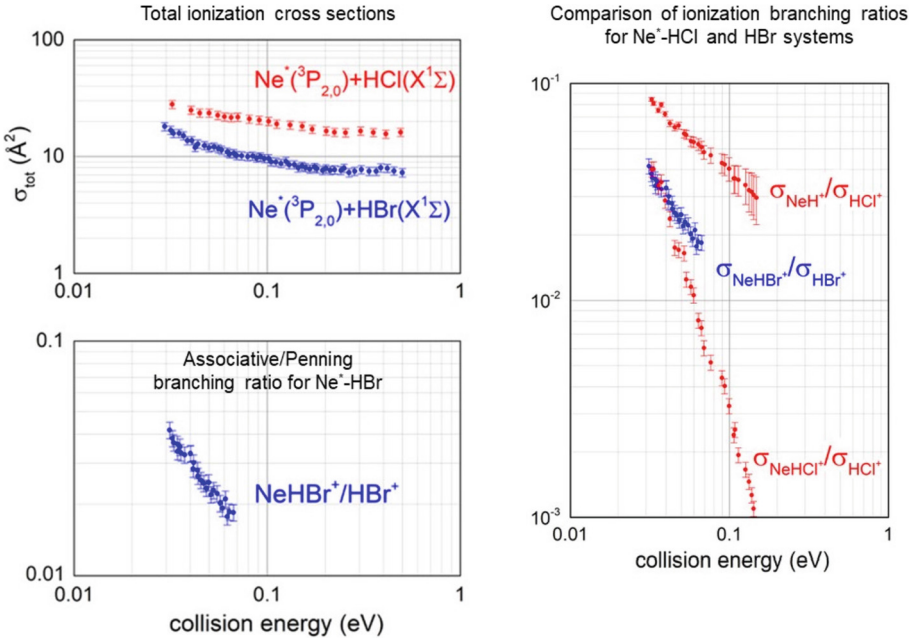

Fig. 2. The comparison between total ionization cross sections (see left-upper panel) and the branching ratios (see left-lower and right panel) recorded for the accessible ionization channels in Ne^* + HX (X = Cl and Br) systems, measured under the same experimental conditions as a function of the collision energy.

From Fig. 2, it can be appreciated that the comparison between the cross sections for the two analyzed systems allows to clearly highlight that for HCl compared to HBr there is a more efficient ionization process in the whole range of the probed collision energies: the ionization cross section is 20 $Å^2$ at a collision energy of 100 meV for Ne^*-HCl, while respect in the case of Ne^*-HBr its value is of about 10 $Å^2$ at the same energy. In addition, the cross sections for HBr show a sharper decrease as the collision energy increases.

Looking at the mass spectrometric data of Eqs. (2)–(4) and (6)–(8), it should be point out that in the case of Ne^*-HCl there is a higher efficiency to react following a proton transfer reaction producing NeH^+ final ions compared to the case of Ne^*-HBr autoionizing collisions. In fact, in Ne^*-HBr autoionization the production of NeH^+ ion is very small as indicated by the relative abundance that is less than 1% at 45 meV of collision energy (see Eq. (7)). Due to this limitation, it was not possible to obtain branching ratios data as a function of the collision energy for the ratio NeH^+/HBr^+ as done in the case of Ne^*-HCl, whose data are reported in the right panel of Fig. 2.

Concerning the data of branching ratios related to associative $(NeHX^+)$/Penning (NeX^+) ionization channels, we can note that the relative probability of the associative ionization is quite similar for the two investigated systems when we are probing the lower portion of the investigated thermal energy range, while for collision energies higher than 45 meV the formation of $NeHCl^+$ ion shows a faster decrease as the collision energy increases respect to $NeHBr^+$.

The total cross sections for Ne^*-HCl and Ne^*-HBr systems in the left-upper panel of Fig. 2 show a decreasing trend as the collision energy increases. This is clear evidence that for both systems the reaction transition state, i.e., $(Ne\cdots HX)^*$, which is the collisional precursor state of entrance channels, is characterized by a strong attraction due to the polarization of outer and floppy cloud of 3*s* external electron of Ne^*. In this way, the interaction between the ionic core of Ne^+ and the permanent electric dipole and quadrupole moments of HCl and HBr molecules is boosted, as can be verified by the data reported in Table 1.

In has to be noted that the symmetry of the molecular orbitals, related to the electron exchange and the electron removing, highlights that in Ne^*-HCl and HBr autoionization reactions, open channels forming different electronic states of the product ions should be strongly stereo-selective. This means that they are promoted by specific angular cones within which the reaction takes place with spatial acceptance and space orientation well-defined. As an example, a representation of angular cones acceptance and orientation is depicted in the left panel of Fig. 3 as determined for the case of the H-end collinear approach of Ne^* atom to HX (X = Cl, Br) molecules, according to the methodology already used in the case of atom-molecule autoionization collisions involving other simple hydrogenated molecules [37, 38]. In the present Ne^*-HX cases, the strong polarization of 3*s* floppy atomic cloud of Ne^* is promoted by the positively charged H atom due to the high electronegativity of the two Cl and Br halogen atoms (see Fig. 3 – left panel). In such a way, this interaction is characterized by a mixing of atomic orbitals having a different symmetry and can stimulate an *indirect* reaction mechanism, which is a pure physical mechanism giving rise to a typical photoionization process. This is realized by the break of the validity of the optical selection rules (which allows the metastability of the Ne^*

Table 1. Ground neutral HCl/HBr and the ionic species HCl^+/HBr^+ in their ground and first excited electronic states: μ (electric dipole moment), Q (electric quadrupole), I (ionization potential), E_A (electron affinity), D_0 (dissociation energy), R_e (equilibrium distance), asymptotic correlation with atomic states and energy levels.

	HCl ($X^1\Sigma^+$)	HBr ($X^1\Sigma^+$)	HCl+ ($X2\Pi_{3/2}$)	HBr+ ($X2\Pi_{3/2}$)	HCl+ ($A2\Sigma_{1/2}$)	HBr+ ($A2\Sigma_{1/2}$)
μ/D	1.103	0.827				
Q/DÅ	3.8	4.3				
I/eV	12.751	11.672				
E_A	< 0	< 0				
D_0/eV	4.434	3.758	4.651	3.900	1.760	1.775
R_e/Å	1.275	1.414	1.315	1.448	1.514	1.684
Asymptotic correlation	$H(^2S_{1/2}) + Cl(^2P_{3/2})$	$H(^2S_{1/2}) + Br(^2P_{3/2})$	$H(^2S_{1/2}) + Cl^+(^3P_2)$	$H(^2S_{1/2}) + Br^+(^3P_2)$	$H^+ + Cl(^2P_{3/2})$	$H(^2S_{1/2}) + Br^+(^1D_2)$
Energy level/eV	0 (reference)	0 (reference)	12.751	11.672	16.272	15.296

atoms) and generates a virtual photon exchange between reagents accompanied by an electron ejection [11, 12].

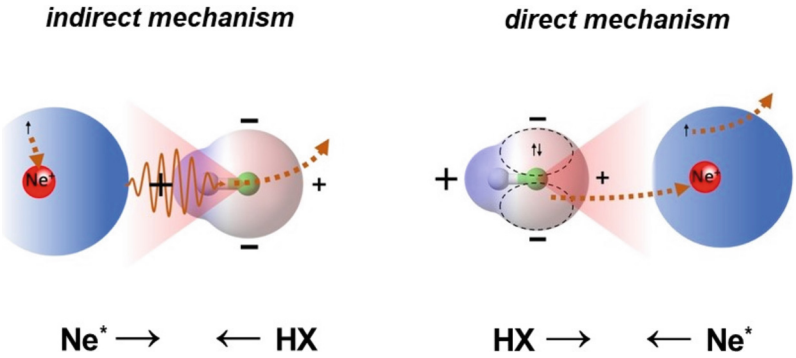

Fig. 3. The schematic view of atomic and molecular orbitals of Ne^* and HX (X = Cl and Br) reagents in a collinear configuration of the autoionizing transition state $(Ne\cdots HX)^*$ evolving to the HX^+ ion formation of in their first excited ($A^2\Sigma$) electronic state. The electronic rearrangements involved are indicated together with the shape of acceptance angular cone for the approach of Ne^* on: (i) the H side of HX molecule (indirect-physical-photoionization mechanism – left panel); (ii) the X side of HX molecule (direct-chemical-oxidation mechanism – right panel).

On the other hand, those collisions where the Ne^* and HX partners are approaching each other along the collinear direction, with Ne^* towards the X atom, are characterize by a different microscopic mechanism which is an oxidation (chemical) mechanism also called *direct mechanism*. In this case, during the collision the HX molecule behaves highlighting its role as a reducing agent. Consequently, the behavior of neon is dominated

by its ionic core (acting as fluorine atom, at short internuclear distances and higher collision energies) so inducing the oxidation of HX via an electron transfer according to the exchange mechanism [12] schematized in the right panel of Fig. 3.

In this way, one electron is ejected from a bonding orbital of HX and this leads to the formation of HX^+ in the first excited ($A^2\Sigma$) electronic state (see Fig. 3), strongly reducing its binding energy value respect to that of the neutral HX state. As a consequence, this favors the dissociation of the HX^+ Penning ion giving rise to the production of NeH^+ by a proton transfer reaction. Analogous situation has been as recently demonstrated in various autoionizing collisions studied at thermal energy, as for example in the case of Ne^*+N_2 reactions [42].

Moreover, possible autoionization processes can be also induced by those collisions between the Ne^* and HX molecules in which the reacting partners are approaching each other in a perpendicular direction. In this case, Penning Ionization Electron Spectroscopy studies, performed in high resolution conditions, have demonstrated that the collisional autoionization involves the formation of the ($X^2\Pi$) ionic ground state of HX^+ which is related to a precursor state [Ne···$HX^+(X^2\Pi)$] having a perpendicular geometry [25–27]. The same PIES spectra, recorded by Hotop group [25, 26] and by Ohno and coworkers [27] clearly show that the formation of the precursor state [Ne···$HX^+(A^2\Sigma)$] in its first excited electronic state preferentially assumes a collinear configuration and will be produced by the two mechanisms shown in Fig. 3.

5 Conclusions

In this article total and partial ionization cross sections are reported and discussed for $Ne^*(^3P_{0,2})$ + HCl and HBr autoionization processes in a comparative analysis pointing out similarities and differences in the microscopic stereodynamics of the two reactions. In the discussion we considered the role of the fundamental interaction components characterizing the autoionizing collision and we were able to distinguish two different microscopic mechanisms (called as *indirect* ad *direct* mechanisms) which are dependent on the stereodynamics of opened ionization channels confined along specific reactive angular cones showing different orientation and acceptance.

Furthermore, the lower efficient autoionization induced by $Ne^*(^3P_{0,2})$ metastable atoms on HBr molecules, respect to that of HCl, is the result of the combination of the following different factors:

a) Polarization effects on Ne^* which trigger the *indirect* reaction mechanism (the physical mechanism depicted in the left panel of Fig. 3); they are attenuated since HBr molecule is less polar with respect to HCl (see the values of dipole moments reported in Table 1);

b) The overlap integral between orbitals of the colliding partners exchanging the electron (Ne^* atoms and HX molecules) tends to reduce since the molecular orbitals of HBr are more diffuse respect to those of HCl;

c) The crucial role of the so called "σ hole" [43–50], localized along HX bond length on the external X part of HX molecules, tends to increase its effect in the case of X = Br; this causes a reduction on the reactivity along the corresponding angular cone of Fig. 3 (right panel) related to the *direct mechanism* (the chemical one) due to the change of the HX molecule polar character.

Acknowledgments. This work was supported and financed with the "Fondo Ricerca di Base, 2018, dell'Università degli Studi di Perugia" (Project Titled: Indagini teoriche e sperimentali sulla reattività di sistemi di interesse astrochimico). Support from Italian MIUR and University of Perugia (Italy) is acknowledged within the program "Dipartimenti di Eccellenza 2018–2022".

References

1. Hotop, H., Illenberger, E., Morgner, H., Niehaus, A.: Chem. Phys. Lett. **10**(5), 493–497 (1971)
2. Siska, P.E.: Rev. Mod. Phys. **65**, 337 (1993)
3. Brunetti, B., Vecchiocattivi, F.: Autoionization dynamics of collisional complexes. In: Ng, C.Y., Baer, T., Powis, I. (eds.) Current Topic on Ion Chemistry and Physics, pp. 359–445. Wiley, New York (1993)
4. Falcinelli, S., Pirani, F., Candori, P., Brunetti, B.G., Farrar, J.M., Vecchiocattivi, F.: Front. Chem. **7**, 445 (2019)
5. Falcinelli, S., Pirani, F., Vecchiocattivi, F.: Atmosphere **6**(3), 299–317 (2015)
6. Alagia, M., Balucani, N., Candori, P., Falcinelli, S., Richter, et al.: Rendiconti Lincei Scienze Fisiche e Naturali **24**, 53–65 (2013)
7. Dulieu, O., Osterwalder, A.: Cold Chemistry, pp. 1–670. Molecular Scattering and Reactivity Near Absolute Zero, Royal Society of Chemistry, Cambridge (2018)
8. Calcote, H.F.: Electrical properties of flames. Symp. Combust. Flame Explos. Phenom. **3**(1), 245–253 (1948)
9. Sugden, T.M.: Excited species in flames. Annu. Rev. Phys. Chem. **13**(1), 369–390 (1962)
10. Falcinelli, S., Vecchiocattivi, F., Pirani, F.: Phys. Rev. Lett. **121**, 163403 (2018)
11. Falcinelli, S., Vecchiocattivi, F., Pirani, F.: Commun. Chem **3**, 64 (2020)
12. Falcinelli, S., Farrar, J.M., Vecchiocattivi, F., Pirani, F.: Acc. Chem. Res. **53**, 2248 (2020)
13. Bettendorff, M., Peyerimhoff, S.D., Buenker, R.J.: Chem. Phys. **66**, 261 (1982)
14. Werner, H.-J., Rosmus, P., Schätzl, W., Meyer, W.: J. Chem. Phys. **80**, 831 (1984)
15. Chapman, D.A., Balasubramanian, K., Sin, S.H.: Phys. Rev. A **38**, 6098 (1988)
16. Candori, P., Falcinelli, S., Pirani, F., Tarantelli, F., Vecchiocattivi, F.: Chem. Phys. Lett. **436**, 322–326 (2007)
17. Snyder, H.L., Smith, B.T., Martin, R.M.: Chem. Phys. Lett. **94**, 90 (1983)
18. de Vries, M.S., Tyndall, G.W., Martin, R.M.: J. Chem. Phys. **80**, 1366 (1984)
19. Tsuji, M., Maier, J.P., Obase, H., Nishimura, Y.: Chem. Phys. **110**, 17–26 (1986)
20. Obase, H., Tsuji, M., Nishimura, Y.: J. Chem. Phys. **87**, 2695–2699 (1987)
21. Simon, W., Yencha, A.J., Ruf, M.-W., Hotop, H.: Z. Phys. D **8**, 71 (1988)
22. Tokue, I., Tanaka, H., Yamasaki, K.: J. Phys. Chem. A **106**, 6068-6074 (2002)
23. Aguilar Navarro, A., Brunetti, B., Falcinelli, S., Gonzalez, M., Vecchiocattivi, F.: J. Chem. Phys. **96**(1), 433–439 (1992)
24. Brunetti, B., Cambi, R., Falcinelli, S., Farrar, J.M., Vecchiocattivi, F.: J. Phys. Chem. **97**(46), 11877-11882 (1993)
25. Yencha, A.J., Ganz, J., Ruf, M.-W., Hotop, H.: Z. Phys. D - Atoms Mol. Clust. **14**, 57–76 (1989)
26. Yencha, A.J., Ruf, M.-W., Hotop, H.: Z. Phys. D - Atoms Mol. Clust. **21**, 113–130 (1991)
27. Imura, K., Kishimoto, N., Ohno, K.: J. Phys. Chem. A **106**, 3759–3765 (2002)
28. Bethe, H.A.: Phys. Rev. **57**, 1125–1144 (1940)
29. Miller, W.H., Morgner, H.: J. Chem. Phys. **67**, 4923–4930 (1977)
30. Gregor, R.W., Siska, P.E.: J. Chem. Phys. **74**, 1078–1092 (1981)
31. Brunetti, B., Candori, P., Falcinelli, S., Pirani, F., Vecchiocattivi, F.: J. Chem. Phys. **139**(16), 164305 (2013)

32. Falcinelli, S., Candori, P., Pirani, F., Vecchiocattivi, F.: Phys. Chem. Chem. Phys. **19**(10), 6933–6944 (2017)
33. Falcinelli, S., Vecchiocattivi, F., Pirani, F.: J. Phys. Chem. A **125**(7), 1461–1467 (2021)
34. Falcinelli, S., Vecchiocattivi, F., Pirani, F.: J. Chem. Phys. **150**(4), 044305 (2019)
35. Nakamura, H.: J. Chem. Phys. Jpn. **26**, 1473–1479 (1969)
36. Miller, W.H.: J. Chem. Phys. **52**, 3563–3572 (1970)
37. Falcinelli, S., Bartocci, A., Cavalli, S., Pirani, F., Vecchiocattivi, F.: Chem. Eur. J. **22**(2), 764–771 (2016)
38. Falcinelli, S., Rosi, M., Cavalli, S., Pirani, F., Vecchiocattivi, F.: Chem. Eur. J. **22**(35), 12518–12526 (2016)
39. Biondini, F., Brunetti, B.G., Candori, P., De Angelis, F., et al.: J. Chem. Phys. **122**(16), 164308 (2005)
40. Brunetti, B., Candori, P., Falcinelli, S., Lescop, B., et al.: Eur. Phys. J. D **38**(1), 21–27 (2006)
41. Brunetti, B.G., Candori, P., Cappelletti, D., Falcinelli, S., et al.: Chem. Phys. Lett. **539–540**, 19–23 (2012)
42. Falcinelli, S., Vecchiocattivi, F., Pirani, F.: Sci. Rep. **11**, 19105 (2021)
43. Falcinelli, S., Vecchiocattivi, F., Farrar, J.M., Brunetti, B.G., Cavalli, S., Pirani, F.: Chem. Phys. Lett. **778**, 138813 (2021)
44. Falcinelli, S., Vecchiocattivi, F., Farrar, J.M., Pirani, F.: J. Phys. Chem. A **125**(16), 3307–3315 (2021)
45. Falcinelli, S., et al.: RSC Adv. **12**, 7587–7593 (2022)
46. Skouteris, D., Balucani, N., Ceccarelli, C., Faginas Lago, N., et al.: MNRAS **482**(3), 3567–3575 (2019)
47. Bartocci, A., Belpassi, L., Cappelletti, D., Falcinelli, S., et al.: J. Chem. Phys. **142**(18), 184304 (2015)
48. Alagia, M., Candori, P., Falcinelli, S., Mundim, M.S.P., Pirani, F., et al.: J. Chem. Phys. **135**(14), 144304 (2011)
49. Alagia, M., Biondini, F., Brunetti, B.G., Candori, P., et al.: J. Chem. Phys. **121**(21), 10508–10512 (2004)
50. Brunetti, B., Candori, P., De Andres, J., Pirani, F., M. Rosi, et al.: J. Phys. Chem. A, **101**(41), 7505–7512 (1997)